Alkene and Alkyne Reactivity over a Metal−Oxo Surface Modeled by Calix[4]arene−Tungsten(IV): Formation of 1-Metallacyclopropene and Alkylidene Complexes

Geoffroy Guillemot, Euro Solari, and Carlo Floriani*

Institut de Chimie Minérale et Analytique, BCH, Université de Lausanne, CH-1015 Lausanne, Switzerland

Nazzareno Re

Facoltà di Farmacia, Università degli Studi "G. D'Annunzio", I-66100 Chieti, Italy

Corrado Rizzoli

Dipartimento di Chimica, Università di Parma, I-43100 Parma, Italy

Received July 17, 2000

This report deals with the deprotonation of [W(η^2-alkene)] complexes to the corresponding 1-metallacyclopropene, which can be equally well obtained via hydride addition to the corresponding [W(η^2-alkyne)]. The ancillary ligand supporting the metal is [*p*-Bu^t-calix[4]-(O)$_4$],$^{4-}$ which mimics an oxo surface. The [W(η^2-2-methyl-2-butene)] complex **2** undergoes deprotonation to give the corresponding anionic 1-metallacyclopropene species **7**. The latter can be protonated back to **2**, alkylated using MeTf to give the corresponding [W(η^2-2,3-dimethyl-2-butene)] complex **3** or metalated at the alkylidene functionality using $ClSnPh_3$ to give **8**. The one-electron oxidation of **7** led to the homolytic cleavage of the W−C bond within the 1-metallacyclopropene unit, thus forming a free radical dimerizing to the dinuclear W−alkylidene **9**. The [W(η^2-alkyne)] complexes **12** and **14** produce the 1-metallacyclopropenes **10** and **16**, respectively, in the reaction with $LiHBEt_3$. The former undergoes reversible protonation−deprotonation to the corresponding [W(η^2-*trans*-stilbene)] derivative **4**, while alkylation using MeTf occurs at one of the oxygens of the calixarene tetraanion, thus forming the neutral metallacyclopropene complex **11**. In the case of a strained alkene, such as acenaphthylene (complex **5**), the deprotonation occurs with the concomitant, homolytic cleavage of a W−C bond and the formation of a free radical alkylidene dimerizing to the ditungsten(V)−dialkylidene species **17**, which has been oxidized using $[Cp_2Fe]^+$ to the corresponding diamagnetic form **18**. The electronic structure and reactivity pathway of the 1-metallacyclopropene functionality has been analyzed using the DFT (density functional theory) approach.

Introduction

Some fundamental steps of alkene and alkyne rearrangements over a metal−oxo surface[1,2] can be nicely modeled by the use of metallacalixarenes.[2] Despite their simplicity, such mononuclear complexes maintain some of the peculiarities of a metal−oxo surface, namely the quasi-planar oxo environment for the metal ion and the bifunctionality of the extended structure.[3−7] This latter property makes available two reaction sites: they are acidic (metal ion) and basic (oxo group) sites. The performance of metallacalixarene in driving key reactions such as dinitrogen reduction,[4] alkylidene forma-

* To whom correspondence should be addressed.

(1) (a) Thomas, J. M.; Thomas, W. J. *Principles and Practice of Heterogeneous Catalysis*; VCH: Weinheim, Germany, 1997. (b) Cox, P. A. *Transition Metal Oxides: An Introduction to their Electronic Structure and Properties*; Oxford University Press: New York, 1992. (c) Gates, B. *Catalytic Chemistry*; Wiley: New York, 1992. (d) *Mechanisms of Reactions of Organometallic Compounds with Surfaces*; Cole-Hamilton, D. J., Williams, J. O., Eds.; Plenum: New York, 1989. (e) Kung, H. H. *Transition Metal Oxides: Surface Chemistry and Catalysis*; Elsevier: Amsterdam, The Netherlands, 1989. (f) Kiselev, V. F.; Krylov, O. V. *Adsorption and Catalysis on Transition Metals and Their Oxides*; Springer: Heidelberg, Germany, 1989. (g) Hoffmann, R. *Solid and Surfaces, A Chemist's View of Bonding in Extended Strucures*, VCH: Weinheim, Germany, 1988. (h) Campbell, I. M. *Catalysis at Surfaces*; Chapman & Hall: London, U.K., 1988. (i) *Catalyst Design, Progress and Perspectives*; Hegedus, L., Ed.; Wiley: New York, 1987. (j) Bond, G. C. *Heterogeneous Catalysis, Principles and Applications*, 2nd ed.; Oxford University Press: New York, 1987.

(2) (a) Corker, J.; Lefebvre, F.; Lecuyer, C.; Dufaud, V.; Quignard, F.; Choplin, A.; Evans, J.; Basset, J.-M. *Science* **1996**, *271*, 966. (b) Niccolai, G. P.; Basset, J.-M. *Appl. Catal., A* **1996**, *146*, 145. (c) Vidal, V.; Theolier, A.; Thivolle-Cazat, J.; Basset, J.-M.; Corker, J. *J. Am. Chem. Soc.* **1996**, *118*, 4595.

(3) Floriani, C. *Chem. Eur. J.* **1999**, *5*, 19.

(4) Caselli, A.; Solari, E.; Scopelliti, R.; Floriani, C.; Re, N.; Rizzoli, C.; Chiesi-Villa, A. *J. Am. Chem. Soc.* **2000**, *122*, 3652.

(5) Caselli, A.; Solari, E.; Scopelliti, R.; Floriani, C. *J. Am. Chem. Soc.* **1999**, *121*, 8296.

(6) (a) Giannini, L.; Caselli, A.; Solari, E.; Floriani, C.; Chiesi-Villa, A.; Rizzoli, C.; Re, N.; Sgamellotti, A. *J. Am. Chem. Soc.* **1997**, *119*, 9198. (b) *Ibid.*, **1997**, *119*, 9709.

(7) (a) Giannini, L.; Solari, E.; Dovesi, S.; Floriani, C. Chiesi-Villa, A.; Rizzoli, C. *J. Am. Chem. Soc.* **1999**, *121*, 2784. (b) Giannini, L.; Guillemot, G.; Solari, E.; Floriani, C. Chiesi-Villa, A.; Rizzoli, C. *J. Am. Chem. Soc.* **1999**, *121*, 2797.

10.1021/om0006155 CCC: $19.00
Publication on Web 11/03/2000

tion from ketones and aldehydes,[5] migration reactions,[6] and olefin rearrangements is well-documented.[7] Following our study on the olefin rearrangements[7b] over a tungstacalixarene oxo surface, we focused on the possibility of discovering a synthetic methodology for intercepting the 1-metallacyclopropene, which paved the way to metallaalkylidenes[8] or other related species.[9,10] This report discusses the general synthesis of alkene and alkyne complexes of W(IV)−calix[4]arene, which have been converted into anionic 1-metallacyclopropene by either deprotonation of the alkene or addition of hydrides to the alkyne. By the use of suitably substituted alkenes and alkynes, 1-metallacyclopropenes have been isolated in stable forms, which do not rearrange to the corresponding alkylidynes. They have been used for studying the reactivity toward electrophiles and one-electron-oxidizing agents. In the former case, the reaction leads to unprecedented substituted alkenes and in the latter to the formation of dinuclear metallaalkylidenes.

Experimental Section

General Procedure. All reactions were carried out under an atmosphere of purified nitrogen. Solvents were dried and distilled before use by standard methods. Infrared spectra were recorded with a Perkin-Elmer FT 1600 spectrophotometer. NMR spectra were recorded on AC-200 and AC-400 Bruker spectrometer. The synthesis of [*cis*-Cl_2{p-Bu^t-calix[4]-$(O)_4$}W] was performed as reported in ref 11.

Computational and Methodological Details. The calculations reported in this paper are based on the ADF (Amsterdam density functional) program package described elsewhere.[12] Its main characteristics are the use of a density fitting procedure to obtain accurate Coulomb and exchange potentials in each SCF cycle, the accurate and efficient numerical integration of the effective one-electron Hamiltonian matrix elements, and the possibility to freeze core orbitals. The molecular orbitals were expanded in an uncontracted triple-ζ Slater-type orbital (STO) basis set for all main-group atoms. For tungsten orbitals, we used a triple-ζ STO basis set for 5s and 5p and for 5d and 6s, as well. As polarization functions, we used one 6p function for tungsten, one 3d for C and O, and one 2p for H. The inner-shell cores have been kept frozen. The LDA exchange correlation potential and energy were used, together with a Vosko−Wilk−Nusair parametrization[13] for homogeneous electron gas correlation, including Becke's nonlocal correction[14] to the local exchange expression and Perdew's nonlocal correction[15] to the local expression of correlation energy. First-order Pauli scalar relativistic corrections[16] were added variationally to the total energy. Molecular structures of all considered complexes were optimized at this nonlocal (NL) level within C_{2v} or C_s symmetry constraints.

Synthesis of 1. Cyclohexene (5.77 g, 70.2 mmol) and Na (0.84 g, 36.7 mmol) were suspended in THF (350 mL) at −50 °C and then degassed (vacuum/N_2 cycles). [*cis*-Cl_2{*p*-Bu^t-calix-[4]-$(O)_4$}W]·2.3C_7H_8 (20.5 g, 18.4 mmol) was added, and the reaction mixture was stirred overnight while slowly warming to room temperature, giving a suspension of a white solid in a brown-red solution. The solid was filtered off, and THF was evaporated to dryness to give a brown-orange residue, which was washed with Et_2O (100 mL) and dried in vacuo to give **1**·$C_4H_{10}O$ (11.04 g, 61%). Anal. Calcd for $C_{54}H_{72}O_5W$: C, 65.85; H, 7.37. Found: C, 65.89; H, 7.37. ^{1}H NMR ($CDCl_3$, 400 MHz, 298 K, ppm): δ 7.11 (s, 8H, Ar H); 4.64 (m, 2H, C_6H_{10}); 4.35 (d, 4H, J = 12.4 Hz, *endo*-CH_2); 4.26 (m, 2H, C_6H_{10}); 4.18 (m, 2H, C_6H_{10}); 3.46 (m, 4H, Et_2O); 3.23 (d, 4H, J = 12.4 Hz, *exo*-CH_2); 1.61 (m, 2H, C_6H_{10}); 1.44 (m, 2H, C_6H_{10}); 1.21 (s, 36H, Bu^t) overlapping with 1.19 (m, 6H, Et_2O).

Synthesis of 2. [*cis*-Cl_2{*p*-Bu^t-calix[4]-$(O)_4$}W]·2.3C_7H_8 (12.2 g, 11.2 mmol) and Na (0.504 g, 21.9 mmol) were suspended in THF (180 mL) at −30 °C, the N_2 atmosphere was purged, and finally 2-methyl-2-butene (11.5 g, 163.4 mmol) was added. The mixture was stirred at −20 °C for 2 days and then allowed to stand at room temperature, giving a suspension of a white solid in a dark red solution. The solid was filtered off, volatiles were evaporated to dryness, toluene (60 mL) was added to the residue, and then volatiles were evaporated again. The residue was dissolved in toluene (200 mL), and the solution was allowed to stand at room temperature for 12 h. A small amount of red solid was filtered off, and the toluene was evaporated to give a dry light-brown solid, which was washed with pentane (80 mL) and dried in vacuo to give **2**·0.5C_7H_8 (6.91 g, 65.1%). Anal. Calcd for $C_{52.5}H_{66}O_4W$: C, 66.73; H, 7.04. Found: C, 66.33; H, 7.00. ^{1}H NMR ($CDCl_3$, 400 MHz, 298 K, ppm): δ 7.26−7.09 (m, 2.5H, tol) overlapping with 7.09 (s, 8H, Ar H); 4.36 (d, 4H, J = 12.3 Hz, *endo*-CH_2); 3.41 (q, 1H, J = 7.1 Hz, $CH_3C(CH_3)C(H)CH_3$); 3.25 (d, 3H, J = 7.1 Hz, $CH_3C(CH_3)C(H)CH_3$); 3.22 (d, 4H, J = 12.3 Hz, *exo*-CH_2); 3.15 (s, 3H, $CH_3C(CH_3)C(H)CH_3$); 3.12 (s, 3H, $CH_3C(CH_3)C(H)CH_3$); 2.34 (s, 1.5H, tol); 1.21 (s, 36H, Bu^t). ^{13}C NMR ($CDCl_3$, 100,6 MHz, 298 K, ppm): δ 91.9 ($CH_3C(CH_3)C(H)CH_3$); 81.2 ($CH_3C(CH_3)C(H)CH_3$, J_{CW} = 30.4 Hz).

Synthesis of 3. Method A. 2,3-Dimethyl-2-butene (1.13 g, 13.43 mmol) and Na (0.165 g, 7.19 mmol) were suspended in THF (110 mL) at −40 °C and then degassed (vacuum/N_2 cycles). [*cis*-Cl_2W(Calix)]·2.3C_7H_8 (4.11 g, 3.69 mmol) was added, and the mixture was stirred overnight, while slowly warming to room temperature, giving a suspension of a white solid in a dark red solution. The solid was filtered off, and THF was evaporated to dryness. Toluene (50 mL) was added to the residue, and then the volatiles were evaporated again. The brown solid was dissolved in toluene (100 mL), and the resulting solution was stirred at room temperature for 4 h. Some red solid was filtered off, and toluene was evaporated to dryness to give a brown residue, which was washed with pentane (50 mL) and dried in vacuo to give **3**·C_5H_{12} (1.6 g, 44%). Anal. Calcd for $C_{55}H_{76}O_4W$: C, 67.06; H, 7.78. Found: C, 66.79; H, 7.98. Crystals suitable for an X-ray analysis were grown from an Et_2O solution.

Method B. A toluene (40 mL) solution of MeTf (0.36 g, 2.19 mmol) was added to a solution of **7**·0.5C_7H_8·0.5C_5H_{12} (2.26 g, 2.29 mmol) in a mixture of THF (80 mL) and dioxane (0.5 mL, 5.87 mmol) at −60 °C and stirred overnight while slowly warming to room temperature. Volatiles of the resulting red brown solution were evaporated to dryness, and toluene (120

(8) (a) Feldman, J.; Schrock, R. R. *Prog. Inorg. Chem.* **1991**, *39*, 1. (b) Schrock, R. R. In *Reactions of Coordinated Ligands*; Braterman, P. S., Ed.; Plenum Press: New York, 1986; Vol. 1. (c) Schrock, R. R. *Acc. Chem. Res.* **1990**, *23*, 158.

(9) (a) Casey, C. P.; Brady, J. T.; Boller, T. M.; Weinhold, F.; Hayashi, R. K. *J. Am. Chem. Soc.* **1998**, *120*, 12500 and references therein. (b) Casey, C. P.; Brady, J. T. *Organometallics* **1998**, *17*, 4620.

(10) (a) Frohnapfel, D. S.; White, P. S.; Templeton. J. L. *Organometallics* **2000**, *19*, 1497. (b) Frohnapfel, D. S.; Enriquez, A. E.; Templeton. J. L. *Organometallics* **2000**, *19*, 221 and references therein. (c) Legzdins, P.; Lumb, S. A.; Rettig, S. J. *Organometallics* **1999**, *18*, 3128.

(11) Giannini, L.; Solari, E.; Floriani, C.; Re, N.; Chiesi-Villa, A.; Rizzoli, C. *Inorg. Chem.* **1999**, *38*, 1438.

(12) (a) Baerends, E. J.; Ellis, D. E.; Ros, P. *Chem. Phys.* **1973**, *2*, 42. (b) Baerends, E. J.; Ros, P. *Chem. Phys.* **1973**, *2*, 51. (c) Baerends, E. J.; Ros, P. *Chem. Phys.* **1975**, *8*, 41. (d) Baerends, E. J.; Ros, P. *Int. J. Quantum Chem.* **1978**, *S12*, 169. (e) Boerrigter, P. M.; te Velde, G.; Baerends, E. J. *Int. J. Quantum Chem.* **1988**, *33*, 87. (f) te Velde, G.; Baerends, E. J. *J. Comput. Phys.* **1992**, *99*, 84. (g) Ziegler, T.; Tschinke, V.; Baerends, E. J.; Snijders, J. G.; Ravenek, W. *J. Phys. Chem.* **1989**, *93*, 3050.

(13) Vosko, S. H.; Wilk, L.; Nusair, M. *Can. J. Phys.* **1980**, *58*, 1200.

(14) Becke, A. D. *Phys. Rev.* **1988**, *A38*, 2398.

(15) Perdew, J. P. *Phys. Rev.* **1986**, *B33*, 8822.

(16) (a) Snijders, J. G.; Baerends, E. J. *Mol. Phys.* **1978**, *36*, 1789. (b) Snijders, J. G.; Baerends, E. J.; Ros, P. *Mol. Phys.* **1979**, *38*, 1909.

mL) was added to give a suspension of a white solid in a red solution. The solid was filtered off, the toluene was evaporated, and the residue was washed with pentane (40 mL) and dried in vacuo to give **3**·C_5H_{12} as a brown solid (1.04 g, 46.1%). Anal. Calcd for $C_{55}H_{76}O_4W$: C, 67.06; H, 7.78. Found: C, 66.97; H, 7.94. ^{1}H NMR ($CDCl_3$, 400 MHz, 298 K, ppm): δ 7.10 (s, 8H, Ar H); 4.38 (d, 4H, J = 12.2 Hz, *endo*-CH_2); 3.23 (d, 4H, J = 12.2 Hz, *exo*-CH_2); 3.14 (s, 12H, $(CH_3)_2CC(CH_3)_2$); 1.27 (m, 6H, pent) overlapping with 1.22 (s, 36H, Bu^t); 0.88 (m, 6H, pent). ^{13}C NMR ($CDCl_3$, 100.6 MHz, 298 K, ppm): δ 88.5 ($(CH_3)_2CC(CH_3)_2$, J_{CW} = 29.5 Hz); 28.1 ($(CH_3)_2CC(CH_3)_2$).

Synthesis of 4. *trans*-Stilbene (1.93 g, 10.7 mmol) and **1**·$C_4H_{10}O$ (10.6 g, 10.7 mmol) were suspended in toluene (170 mL) and the mixture heated at 60 °C for 10 h to give a dark red-brown suspension. Some solid was filtered off the warm mixture. Volatiles were removed in vacuo, and *n*-pentane (80 mL) was added to the brown residue. The solution was cooled to −20 °C, yielding 5.62 g (5.33 mmol, 50%) of **4**·0.5C_7H_8. Anal. Calcd for $C_{61.5}H_{68}O_4W$: C, 70.01; H, 6.50. Found: C, 69.96; H, 6.80. ^{1}H NMR ($CDCl_3$, 400 MHz, 298 K, ppm): δ 7.52 (m, 4H, Ar H (stilbene)); 7.35 (m, 4H, Ar H (stilbene)); 7.10−7.05 (m, 2.5H, tol) overlapping with 7.05 (s, 8H, Ar H); 6.91 (m, 2H, Ar H (stilbene)); 4.79 (s, 2H, PhC*H*C*H*Ph); 3.93 (d, 4H, J = 12.3 Hz, *endo*-CH_2); 3.02 (d, 4H, J = 12.3 Hz, *exo*-CH_2); 2.35 (s, 1.5H, tol); 1.17 (s, 36H, Bu^t). ^{13}C NMR ($CDCl_3$, 100.6 MHz, 298 K, ppm): δ 82.3 (W(Ph*C*HCHPh), J_{CW} = 27 Hz). The X-ray structure has been established for this compound, analyzed as the acetonitrile adduct, from a solution in CD_3CN.

Synthesis of 5. Acenaphthylene (1.34 g, 8.79 mmol) and **1**·$C_4H_{10}O$ (8.01 g, 8.13 mmol) were suspended in THF (220 mL), and the reaction mixture was heated at 60 °C for 1 h. This brown suspension was filtered, and volatiles of the resulting brown-red solution were evaporated to dryness, giving a brown solid which was washed with Et_2O (55 mL) and dried in vacuo to yield 6.86 g (80%) of **5**·$C_4H_{10}O$. Anal. Calcd for $C_{60}H_{70}O_5W$: C, 68.31; H, 6.69. Found: C, 68.57; H, 6.70. ^{1}H NMR ($CDCl_3$, 400 MHz, 298 K, ppm): δ 7.64 (m, 2H, Ar H (acenaphthylene)); 7.37 (m, 2H, Ar H (acenaphthylene)); 7.08 (m, 2H, Ar H (acenaphthylene)); 7.00 (s, 8H, Ar H); 5.67 (s, 2H, C*H*═C*H*); 4.04 (d, J = 12.4 Hz, 4H, *endo*-CH_2); 3.47 (m, 4H, Et_2O); 3.07 (d, J = 12.4 Hz, 4H, *exo*-CH_2); 1.16 (s, Bu^t overlapping with m, Et_2O).

Synthesis of 6. 1·$C_4H_{10}O$ (6.69 g, 6.79 mmol) was added to a solution of norbornene (0.63 g, 6.70 mmol) in toluene (170 mL), and the mixture was stirred at 60 °C for 24 h. A small amount of solid was filtered off from the resulting brown solution. Volatiles were evaporated to dryness to give a brown grayish solid, which was washed with *n*-pentane (50 mL) and dried in vacuo to yield 3.4 g (52.3%) of **6**·0.5C_5H_{12}. Anal. Calcd for $C_{53.5}H_{68}O_4W$: C, 67.01; H, 7.15. Found: C, 67.12; H, 6.99. ^{1}H NMR (C_6D_6, 200 MHz, 298 K, ppm): δ 7.07 (s, 8H, Ar H); 4.83 (s, 2H, C*H*═C*H*); 4.65 (d, 4H, J = 12.2 Hz, *endo*-CH_2); 3.47 (s, 2H, C*H*); 3.21 (d, 4H, J = 12.2 Hz, *exo*-CH_2); 2.24 (m, 2H, CH_2CH_2); 1.55 (m, 2H, CH_2CH_2); 1.22 (m, 3H, pent); 1.10 (s, 36H, Bu^t, overlapping with m, 1H, CH_2); 0.87 (m, 3H, pent); 0.76 (m, 1H, CH_2). Crystals suitable for an X-ray analysis were grown from a toluene/pentane solution.

Synthesis of 7. LiBu (3.2 mL, 2.12 *N*, 6.78 mmol) was added to a toluene (180 mL) solution of **2**·0.5C_7H_8 (6.75 g, 7.15 mmol) at −70 °C and stirred overnight, while slowly warming to room temperature. Volatiles of the resulting red-violet suspension were evaporated to dryness, and the red-violet residue was washed with *n*-pentane (80 mL) and then dried in vacuo to give **7**·0.5C_7H_8·0.5C_5H_{12} (4.84 g, 69.7%). Anal. Calcd for $C_{55}H_{71}LiO_4W$: C, 66.93; H, 7.25. Found: C, 66.85; H, 7.32. ^{1}H NMR (Pyr-d_5, 400 MHz, 298 K, ppm): δ 7.32−7.15 (m, 2.5H, tol) overlapping with 7.24 (s, 8H, Ar H); 5.30 (m, 4H, *endo*-CH_2) overlapping with 5.23 (br, 3H, C_5H_9); 3.67−3.17 (br, 6H, C_5H_9) overlapping with 3.37 (m, 4H, *exo*-CH_2); 2.20 (s, 1.5H, tol); 1.21 (s, 36H, Bu^t) overlapping with 1.17 (m, 3H, pent); 0.80 (m, 3H, pent). ^{1}H NMR (Pyr-d_5, 400 MHz, 263 K, ppm): δ 7.32−7.12 (m, 2.5H, tol) overlapping with 7.23 (s, 8H, Ar H); 5.31 (d, 4H, J = 11.4 Hz, *endo*-CH_2); 5.28 (s, 3H, $CH_3CC(CH_3)_2$); 3.42 (s, 6H, $CH_3CC(CH_3)_2$); 3.35 (d, 4H, J = 11.4 Hz, *exo*-CH_2); 2.14 (s, 1.5H, tol); 1.17 (s, 36H, Bu^t) overlapping with 1.14 (m, 3H, pent); 0.72 (m, 3H, pent). ^{13}C NMR (TDF, 100.6 MHz, 253 K, ppm): δ 271.0 ($CH_3CC(CH_3)_2$, J_{CW} = 84.4 Hz); 52.4 ($CH_3CC(CH_3)_2$). Crystals suitable for an X-ray analysis were grown from a THF/diglyme solution. Reaction of **7**·0.5C_7H_8·0.5C_5H_{12} with a stoichiometric amount of PyHCl in toluene at room temperature led to the starting material **2**·0.33C_7H_8, as determined by ^{1}H NMR.

Synthesis of 8. Ph_3SnCl (1.38 g, 3.58 mmol) and **7**·0.5C_7H_8·0.5C_5H_{12} (3.54 g, 3.59 mmol) were suspended in a mixture of THF (150 mL) and dioxane (0.8 mL, 9.39 mmol) and stirred overnight at room temperature. Volatiles of the resulting dark red solution were evaporated to dryness, and toluene (100 mL) was added to give a brown suspension, which was stirred for 2 h at room temperature. A white solid was filtered off, and toluene was removed in vacuo to give a brown product which was washed with *n*-pentane (40 mL) and dried in vacuo to give **8**·C_5H_{12} (3.04 g, 64.2%). Anal. Calcd for $C_{72}H_{88}O_4SnW$: C, 65.51; H, 6.72. Found: C, 65.55; H, 6.64. ^{1}H NMR (C_6D_6, 400 MHz, 298 K, ppm): δ 7.94−7.81 (m, 6H, $(C_6H_5)_3Sn$); 7.13−7.03 (m, 9H, $(C_6H_5)_3Sn$); 6.99 (m, 4H, Ar H); 6.96 (m, 4H, Ar H); 4.50 (d, 4H, J = 12 Hz, *endo*-CH_2); 3.97 (s, 3H, $(CH_3)_2CC(CH_3)SnPh_3$, J_{HSn} = 61.6 Hz); 3.63 (s, 3H, $(CH_3)_2CC(CH_3)SnPh_3$); 3.47 (s, 3H, $(CH_3)_2CC(CH_3)SnPh_3$); 3.05 (d, 4H, J = 12 Hz, *exo*-CH_2); 1.25 (m, 6H, pentane); 1.07 (s, 36H, Bu^t); 0.87 (m, 6H, pentane). Crystals suitable for an X-ray analysis were grown from a toluene/pentane solution.

Synthesis of 9. CuCl (0.176 g, 1.778 mmol) was added to a solution of **7**·0.5C_7H_8·0.5C_5H_{12} (1.75 g, 1.77 mmol) in THF (100 mL) at room temperature. The reaction mixture was degassed and saturated with CO (vacuum/CO cycles) and then stirred overnight at room temperature. The resulting red solution was separated from a copper metallic mirror and a reddish brown product. Volatiles were evaporated to dryness, and toluene (80 mL) was added to give a red suspension. A red-orange solid was filtered off at 70 °C, and toluene was evaporated to give a light brown solid that was washed with Et_2O (40 mL) and dried in vacuo to yield 0.79 g of **9**·$C_4H_{10}O$ (45.8%). Anal. Calcd for $C_{106}H_{142}O_{10}W_2$: C, 65.49; H, 7.36. Found: C, 65.05; H, 7.38. ^{1}H NMR ($CDCl_3$, 200 MHz, 298 K, ppm): δ 7.09 (s, 8H, Ar H); 5.96 (s, 3H, C(CH_3)); 4.56 (d, 4H, J = 12.7 Hz, *endo*-CH_2); 3.47 (m, 4H, Et_2O); 3.25 (d, 4H, J = 12.7 Hz, *exo*-CH_2); 2.00 (s, 6H, $C(CH_3)_2$); 1.23−1.16 (m, 6H, Et_2O overlapping with s, 36H, Bu^t). ^{13}C NMR ($CDCl_3$, 100.6 MHz, 298 K, ppm): δ 301.15 (W═C); 60.42 (W═C(CH_3)*C*(CH_3)$_2$); 29.73 (WC(CH_3)C(*C*H_3)$_2$); 27.80 (W═C(*C*H_3)).

Synthesis of 10. Method A. LiBu (3.2 mL, 1.85 *N*, 5.92 mmol) was added to a toluene (240 mL) solution of **4**·0.5C_7H_8 (6.3 g, 5.97 mmol) at −70 °C and stirred overnight while slowly warming to room temperature. Volatiles of the resulting red suspension were evaporated, and the brown reddish residue was washed with *n*-pentane (70 mL) and dried in vacuo to give **10**·C_7H_8 (2.74 g, 41%). Anal. Calcd for $C_{65}H_{71}LiO_4W$: C, 70.52; H, 6.46. Found: C, 70.66; H, 6.70. ^{1}H NMR (CD_3CN, 400 MHz, 298 K, ppm): δ 7.64 (m, 2H, $C_{14}H_{11}$); 7.49 (m, 2H, $C_{14}H_{11}$); 7.23−7.07 (m, 5H, $C_{14}H_{11}$ overlapping with 5H, tol); 7.03 (s, 8H, Ar H); 6.67 (m, 1H, $C_{14}H_{11}$); 6.59 (m, 1H, $C_{14}H_{11}$); 4.36 (d, 4H, J = 11.2 Hz, *endo*-CH_2); 2.94 (d, 4H, J = 11.2 Hz, *exo*-CH_2); 2.32 (s, 3H, tol); 1.14 (s, 36H, Bu^t). ^{13}C NMR (CD_3CN, 100.6 MHz, 298 K, ppm): δ 253.14 (W*C*PhCHPh, J_{CW} = 88 Hz); 72.04 (W*C*HPhCPh). Crystals suitable for a preliminary X-ray analysis were grown from a THF/*n*-heptane solution. Reaction of **10**·C_7H_8 with a stoichiometric amount of PyHCl in toluene at room temperature led to the starting material **4**·0.5C_7H_8, as determined by ^{1}H NMR.

Method B. A solution of $LiHBEt_3$ (2.45 mL, 1 *N* in THF, 2.45 mmol) in THF (40 mL) was added to a suspension of **12**·0.5C_7H_8·0.5C_6H_{14} (2.95 g, 2.69 mmol) in THF (80 mL) at −50

°C. The mixture was stirred overnight while slowly warming to room temperature. The resulting brown reddish solution was filtered. Volatiles were evaporated to dryness to give a red solid that was washed with *n*-hexane (30 mL) and dried in vacuo to yield 1.97 g of **10**·2C_4H_8O·0.5C_6H_{14} (60.8%). Anal. Calcd for $C_{69}H_{86}LiO_6W$: C, 68.94; H, 7.21. Found: C, 68.90; H, 7.33. ^{1}H NMR (CD_3CN, 400 MHz, 298 K, ppm): δ 7.61 (m, 2H, $C_{14}H_{11}$); 7.46 (m, 2H, $C_{14}H_{11}$); 7.23−7.07 (m, 5H, $C_{14}H_{11}$); 7.01 (s, 8H, Ar H); 6.64 (m, 1H, $C_{14}H_{11}$); 6.57 (m, 1H, $C_{14}H_{11}$); 4.36 (d, J = 11.2 Hz, 4H, *endo*-CH_2); 3.64 (m, 8H, THF); 2.94 (d, J = 11.2 Hz, 4H, *exo*-CH_2); 1.80 (m, 8H, THF); 1.20 (m, hex) overlapping with 1.15 (s, 36H, Bu^t); 0.89 (m, 3H, hexane). ^{13}C NMR (CD_3CN, 100.6 MHz, 298 K, ppm): δ 253.2 (W*C*Ph-CHPh, J_{CW} = 88 Hz); 72 (W*C*HPhCPh). Crystals suitable for an X-ray analysis were grown in THF/pentane solution.

Synthesis of 11. MeTf was added, in a 1:1 molar ratio, to a suspension of **10** in toluene at −60 °C and stirred overnight while slowly warming to room temperature. A light brown solid was filtered off. Volatiles were evaporated to dryness and pentane added. Complex **11** was isolated in low yield as a microcrystalline red compound and characterized by 1D and 2D NMR experiments. ^{1}H NMR (Tol-d_8, 400 MHz, 298 K, ppm): δ 8.02 (m, 2H, Ar H (stilbene)); 7.59 (m, 3H, Ar H (stilbene)); 7.30−6.70 (m, Ar H (stilbene), Ar H (tol)); 4.73 (d, ^{1}H, CH_2); 4.44 (d, 1H, CH_2); 4.23 (d, 1H, CH_2); 3.62 (s, 3H, calix[4]-(O)$_3$(OCH_3)); 3.48 (d, 1H, CH_2); 3.26 (d, 1H, CH_2); 3.20 (d, 1H, CH_2); 3.04 (d, 1H, CH_2); 2.74 (d, 1H, CH_2); 1.43 (s, 18H, Bu^t); 0.80 (s, 9H, Bu^t); 0.74 (s, 9H, Bu^t). ^{13}C NMR (Tol-d_8, 100.6 MHz, 298 K, ppm): δ 272.21 (W*C*PhCHPh); 69.42 (calix[4]-(O)$_3$(O*C*H$_3$)).

Synthesis of 12. 1·$C_4H_{10}O$ (8.95 g, 9.09 mmol) was added to a solution of diphenylacetylene (1.62 g, 9.09 mmol) in toluene (150 mL) at room temperature. The reaction mixture was irradiated for 17 h with a Xe lamp (540 W/m^2 at 340 nm). The toluene of the resulting brown-red suspension was removed in vacuo and added again (150 mL). A small amount of solid was filtered off, and toluene was evaporated to dryness to give a brown solid, which was washed with *n*-hexane (100 mL) and dried in vacuo to give **12**·0.5C_7H_8·0.5C_6H_{14} (5.89 g, 59.1%). Anal. Calcd for $C_{64.5}H_{73}O_4W$: C, 70.68; H, 6.71. Found: C, 70.56 H, 6.53. ^{1}H NMR (C_6D_6, 400 MHz, 298 K, ppm): δ 8.57 (m, 4H, C_2(C_6H_5)$_2$); 7.34 (m, 4H, C_2(C_6H_5)$_2$); 7.15 (m, C_2(C_6H_5)$_2$ overlapping with signal from deuterated solvent); 7.08 (s, 8H, Ar H); 7.05−6.95 (m, 2.5H, tol); 4.80 (d, J = 12.2 Hz, 4H, *endo*-CH_2); 3.19 (d, J = 12.2 Hz, 4H, *exo*-CH_2); 2.11 (s, 1.5H, toluene); 1.23 (m, 4H, hexane); 1.11 (s, 36H, Bu^t); 0.88 (m, 3H, hexane). ^{13}C NMR (C_6D_6, 100.6 MHz, 298 K, ppm): δ 189.5 (*C*$_2$(C_6H_5)$_2$). Crystals suitable for an X-ray analysis were obtained by hexane solutions at room temperature.

Synthesis of 13. 1·$C_4H_{10}O$ (4.54 g, 4.61 mmol) was added to a solution of 2-butyne (0.69 g, 12.75 mmol) in toluene (180 mL) at −70 °C. The solution was irradiated for 24 h with a Xe lamp (540 W/m^2 at 340 nm). The resulting brown reaction mixture was filtered, and toluene was removed in vacuo. The pale green residue was taken up and washed in *n*-hexane (250 mL), collected, and dried in vacuo (3.23 g (77%). Anal. Calcd for **13**·0.5C_7H_8 ($C_{51.5}H_{62}O_4W$): C, 66.59; H, 6.73. Found: C, 66.51; H, 6.86. ^{1}H NMR (C_6D_6, 200 MHz, 298 K, ppm): δ 7.11 (s, 8H, Ar H overlapping with m, tol); 4.65 (d, J = 12.2 Hz, 4H, *endo*-CH_2); 3.26 (s, 6H, (*C*H$_3$)CC(*C*H$_3$)) overlapping with 3.25 (d, J = 12.2 Hz, 4H, *exo*-CH_2); 2.10 (s, 1.5H, tol); 1.12 (s, 36H, Bu^t). ^{13}C NMR (C_6D_6, 52 MHz, 298 K, ppm): δ 189.5 ((CH$_3$)*CC* (CH$_3$)).

Synthesis of 14. 1·C_4H_8O (3.13 g, 3.18 mmol) was added to a solution of 1-phenyl-1-propyne (0.53 g, 4.61 mmol) in toluene (100 mL) at room temperature. The reaction mixture was stirred at 60 °C for 16 h. Volatiles of the resulting red suspension were evaporated to dryness. The microcrystalline orange residue was washed with *n*-pentane (35 mL) and dried in vacuo (2.49 g, 80%). Anal. Calcd for **14**·0.5C_5H_{12} ($C_{55.5}H_{66}O_4W$): C, 67.95; H, 6.78. Found: C, 68.21; H, 6.95. ^{1}H NMR (C_6D_6, 400 MHz, 298 K, ppm): δ 8.64 (m, 2H, (C_6H_5)CC(CH$_3$)); 7.38 (m, 2H, (C_6H_5)CC(CH$_3$)); 7.20 (m, 1H, (C_6H_5)CC(CH$_3$)); 7.09 (s, 8H, Ar H); 4.73 (d, J = 12.4 Hz, 4H, *endo*-CH_2); 3.49 (s, 3H, (C_6H_5)CC(CH$_3$)); 3.24 (d, J = 12.4 Hz, 4H, *exo*-CH_2); 1.20 (m, 3H, pent); 1.11 (s, 36H, Bu^t); 0.87 (m, 3H, pent). ^{13}C NMR (C_6D_6, 100.6 MHz, 298 K, ppm): δ 197.1 ((C_6H_5)*C*C(CH$_3$)); 184 ((C_6H_5)C*C*(CH$_3$)); 15.4 ((C_6H_5)-CC(*C*H$_3$)).

Synthesis of 15. 1·$C_4H_{10}O$ (5.82 g, 5.91 mmol) was added to a THF solution of phenylacetylene (0.61 g, 5.95 mmol) at room temperature, and the mixture was stirred overnight. Some red-purple solid was filtered off, and volatiles of the resulting red solution were evaporated to dryness. The brown residue was washed with *n*-pentane (65 mL) and dried in vacuo (2.37 g, 40%). Anal. Calcd for **15**·C_4H_8O ($C_{56}H_{66}O_5W$): C, 67.06; H, 6.63. Found: C, 66.94; H, 6.56. ^{1}H NMR (C_6D_6, 400 MHz, 298 K, ppm): δ 12.43 (br, ^{1}H, C_6H_5C*H*); 8.66 (m, 2H, C_6H_5-CCH); 7.32 (m, 2H, C_6H_5CCH); 7.16 (m, 1H, (C_6H_5)CCH overlapping with signal of the deuterated solvent); 7.09 (s, 8H, Ar H); 4.77 (d, J = 12.4 Hz, 4H, *endo*-CH_2); 3.52 (m, 4H, THF); 3.22 (d, J = 12.4 Hz, 4H, *exo*-CH_2); 1.40 (m, 4H, THF); 1.10 (s, 36H, Bu^t).

Synthesis of 16. 14·0.5C_7H_8·C_5H_{12} (1 g, 0.941 mmol) was added to a solution of LiHBEt$_3$ (0.98 mL, 1 *N* in THF, 0.98 mmol) in THF (80 mL) at −60 °C. The mixture was stirred overnight while slowly warming to room temperature. Volatiles were evaporated to dryness, and the brown reddish residue was washed with *n*-pentane (30 mL) and dried in vacuo (0.49 g, 40%). Anal. Calcd for **16**·3C_4H_8O·0.5C_5H_{12} ($C_{67.5}H_{91}$-LiO_7W): C, 67.27; H, 7.61. Found: C, 67.33; H, 7.59. ^{1}H NMR (Pyr-d_5, 400 MHz, 298 K, ppm): δ 8.31 (m, 2H, C_6H_5CC(H)-CH$_3$); 7.62 (m, 2H, C_6H_5CC(H)CH$_3$); 7.28 (s, 8H, Ar H); 6.76 (m, 1H, C_6H_5CC(H)CH$_3$); 6.46 (q, J = 5.4 Hz, 1H, C_6H_5CC(*H*)-CH$_3$); 5.26 (d, J = 11.6 Hz, 4H, *endo*-CH_2); 3.64 (m, 12H, THF); 3.48 (d, J = 5.4 Hz, 3H, C_6H_5CC(H)*C*H$_3$); 3.40 (d, J = 11.6 Hz, 4H, *exo*-CH_2); 1.61 (m, 12H, THF); 1.21 (s, 36H, Bu^t overlapping with m, pentane); 0.80 (m, 3H, pentane). ^{13}C NMR (Pyr-d_5, 700.6 MHz, 298 K, ppm): δ 255 (W*C*PhC(H)Me). Crystals for a preliminary X-ray analysis were grown in a THF/TMEDA solution.

Synthesis of 17. LiBu (3.3 mL, 1.67 *N*, 5.51 mmol) was added to a toluene (250 mL) suspension of **5**·$C_4H_{10}O$ (6.2 g, 5.87 mmol) at −60 °C and stirred overnight while slowly warming to room temperature. Volatiles of the resulting dark red solution were evaporated to dryness, and Et_2O (210 mL) was added. The resulting solution was allowed to stand at room temperature for 1 day. Some solid was filtered off, volatiles were evaporated again to dryness, and DME (10 mL) and *n*-hexane (50 mL) were added to the residue to give a red microcrystalline suspension, which was isolated and dried in vacuo (4.0 g, 52.4%). Anal. Calcd for **17**·6$C_4H_{10}O_2$·C_6H_{14} ($C_{142}H_{192}Li_2O_{20}W_2$): C, 65.58; H, 7.44. Found: C, 65.64; H, 7.53. μ_{eff} = 1.59 μ_B at 298 K. Crystals suitable for an X-ray analysis were obtained from a THF solution.

Synthesis of 18. [Cp_2FeBPh_4] (66.4 mg, 0.132 mmol) was added to a solution of **17**·6$C_4H_{10}O_2$·C_6H_{14} (164 mg, 0.126 mmol) in toluene (60 mL) at −10 °C and stirred overnight at the same temperature. The reaction mixture was then allowed to return to room temperature, and dioxane (0.5 mL) was added. The suspension was stirred for 1 h, and a white solid was filtered off. Volatiles of the resulting red solution were evaporated to dryness, and the red residue was washed with pentane (15 mL) to yield 80 mg of **18**. ^{1}H NMR (Pyr-d_5, 400 MHz, 298 K, ppm): δ 10.36 (s, 1H, W=CC(*H*)); 8.50 (m, 1H, Ar H (acenaphthylene)); 7.84 (m, 2H, Ar H (acenaphthylene)); 7.40 (m, 9H, Ar H (calix) overlapping with Ar H (acenaphthylene)); 7.10 (m, 1H, Ar H (acenaphthylene)); 6.85 (m, 1H, Ar H (acenaphthylene)); 4.97 (d, J = 12.1 Hz, 4H, *endo*-CH_2); 3.39 (d, J = 12.1 Hz, 4H, *exo*-CH_2); 1.21 (s, 36H, Bu^t). ^{13}C NMR (Pyr-d_5, 100.6 MHz, 298 K, ppm): δ 284.4 (W=CC(H)); 65.9 (W=CC-

(H)). Crystals suitable for an X-ray analysis were grown in a toluene/*n*-heptane solution.

X-ray Crystallography for Complexes 3, 4, 7, 8, 10, 12, 17, and 18. Single crystals suitable for X-ray diffraction were grown from common organic solvents (Table 1). Data for **8**, **10**, **17**, and **18** were collected on a Mar345 image plate, while those for **3**, **4**, **7**, and **12** were collected on a Kuma CCD using Mo Kα radiation. The solutions and refinements were carried out using the programs SHELX76[17] and SHELX93.[18] The details of the X-ray data collection, structure solutions, and refinements are given in the Supporting Information.[19]

Results and Discussion

(A) Synthesis and Reactivity. Scheme 1 summarizes the two synthetic methods leading to the formation of alkene-W(IV)-calix[4]arene complexes. Compounds **1**−**3** have been obtained by reducing [*cis*-Cl_2{*p*-Bu^t-calix[4]-$(O)_4$}W][11] with sodium metal in the presence of the corresponding olefin. For those alkenes which cannot be used in the presence of sodium metal for a variety of reasons, the synthesis of the alkene complex was performed via a thermally or photochemically assisted displacement of cyclohexene from complex **1**. With such a procedure complexes **4**−**6** have been synthesized. The alkene complexes in Scheme 1 have been fully characterized, and two of them, **1** and **4**, have been briefly mentioned in a recent report.[7b] The solution characterization of all of them by ^{1}H NMR spectroscopy showed the presence of a 4-fold symmetry calixarene moiety (a single pair of doublets for the bridging methylenes and a singlet for the Bu^t groups), while a 2-fold symmetry is expected on the basis of the solid-state structure. The [{*p*-Bu^t-calix[4]-$(O)_4$}W] fragment has two d_{xz} and d_{yz} degenerate bonding orbitals, which are equally available for the back-bonding to the C═C unit.[7b] On the basis of our DFT calculations (see below), the energy barrier between the two isoenergetic positions at 90° to each other is so low (5.7 kcal mol^{-1}) that alkene free rotation is possible around the *z* axis.

The solid-state structures of **3**, **4**, and **6** have been determined, though details are given only for 3 and 4 (Figures 1 and 2), the structure of **6** being available in the Supporting Information. The structural analysis of **4** has been carried out on the solvated form containing an acetonitrile inside the cavity bonded to the metal. The most common structural and conformational parameters are listed in Tables 2 and 5, respectively. Although the structural parameters support the metallacyclopropane formulation, there is a significant difference between **3** and **4**·MeCN, due to the presence of the acetonitrile at the metal. In the latter case, a significant shortening of the C−C bond is observed, from 1.476(13) (**3**) to 1.37(2) Å (**4**). The W−C bond has a quite strong σ character (2.160(4) Å (av)). The plane of the olefin C_2 unit is nearly perpendicular to the mean O_4 plane, the dihedral angles being 90.9(3) and 91.0(5)°, respectively, for **3** and **4**. The O_4 core shows a significant dihedral distortion in **3**, while it is almost planar in **4**. This results from changes in the conformation of the calixarene fragment, from an elliptical to a spherical cone shape moving from **3** to **4** (Table 5), as a consequence of the acetonitrile binding at the metal in **4**. The metal behaves in the former case as if it has a *cis*-L_2MO_4 coordination environment and a *trans* environment, *trans*-L_2MO_4, in the case of **4**. In complex **3**, the four W−O bond lengths appear in pairs with W−O1 and W−O3 (1.844(7) Å (av)) being much shorter than W−O2 and W−O4 (2.023(2) Å) due to a single d_π orbital available at the metal for the donation from the oxygens of the calixarene, the other one being involved in π back-donation to the olefin.[7b] In the case of **4**, the four W−O bond distances fall in a rather narrow range (Table 2).

The deprotonation of the W−alkene functionality has been carried out on **2**, which has three methyl substituents at the C═C bond, to prevent any rearrangement of the 1-metallacyclopropene to the corresponding alkylidyne.[7b] The reaction of **2** with LiBu led to the 1-metallacyclopropene **7** (Scheme 2), which was isolated in 70% yield. The alkylidene **7**, a very stable compound, was characterized both in solution and in the solid state. The ^{1}H NMR spectrum shows a 4-fold symmetry calixarene skeleton for the reasons outlined above, while the ^{13}C NMR spectrum contains a resonance at 271.0 ppm for the alkylidene carbon. The solid-state structure of **7** will be reported jointly with that of **10**.

Complex **7** is very susceptible to electrophilic attack, as reported in Scheme 2. The protonation with PyHCl returns **7** to **3**. In this reaction, we cannot exclude the assistance of one of the oxygens, as the primary site of the protonation. The alkylation with MeTf occurs at the alkylidene carbon as well, forming the 2,3-dimethyl-2-butene−W derivative **3**, which was obtained also by the direct synthesis given in Scheme 1. The metalation with Ph_3SnCl follows the same pathway, leading to the tin derivative **8**, which can be a useful material in transmetalation reactions. Its solid-state structure is shown in Figure 3, while the structural and conformational parameters are listed in Tables 2 and 5, respectively. They are not that different from those of the aforementioned alkene complexes **3** and **4**, which we refer to for a detailed description of the structure.

The anionic 1-metallacyclopropene **7** undergoes one-electron oxidation by a variety of reagents, the best one being [CuCl] followed by CO. The reaction proceeds with the formation of a copper metal mirror and **9**. The formation of **9** suggests the intermediacy of a free-radical species such as **A** (Scheme 2), preferentially undergoing the dimerization rather than causing the hydrogen abstraction from the solvent. We do not have, in fact, any evidence of the formation of an alkylidene coming from the latter route, even in trace amounts. The removal of one electron from **7** gave a free-radical type metallacyclopropane undergoing the W−C homolytic cleavage at the most substituted carbon, as supported by the DFT calculations (see below). The structure of **9** is fully supported by the analytical and spectroscopic data (see Experimental Section) and is quite similar to that of **17**, which will be described later on in this report. A detailed theoretical analysis is given at the end of this section on the genesis of **9**, from one-electron oxidation of **7**.

A different synthetic access to 1-metallacyclopropene, which can be a versatile organometallic synthon, is displayed in Scheme 3. The mono(alkyne) derivatives

(17) Sheldrick, G. M. SHELX76, Program for Crystal Structure Determination; University of Cambridge, Cambridge, England, 1976.
(18) Sheldrick, G.M. SHELXL93, Program for Crystal Structure Refinement; University of Göttingen, Göttingen, Germany, 1993.
(19) See paragraph at the end of paper regarding the Supporting Information.

Table 1. Experimental Data for the X-ray Diffraction Studies on Crystalline Complexes 3, 4, 7, 8, 10, 12, 17, and 18

	3	**4**	**7**	**8**	**10**	**12**	**17**	**18**
formula	$C_{50}H_{64}O_4W\cdot 2C_4H_{10}O$	$C_{60}H_{64}D_3NO_4W$	$C_{49}H_{61}O_4W\cdot C_{12}H_{28}LiO_6\cdot 3C_4H_8O$	$C_{67}H_{76}O_4SnW\cdot C_4H_{10}O$	$C_{66}H_{79}LiO_6W\cdot 1.5C_4H_{10}O$	$C_{58}H_{62}O_4W\cdot 0.25C_{14}H_{10}$	$C_{128}H_{150}Li_2O_{12}W_2\cdot 6C_4H_8O$	$C_{112}H_{118}O_8W_2\cdot 5.5C_4H_8O$
a, Å	12.399(2)	12.844(2)	17.292(2)	17.748(2)	14.696(3)	12.976(3)	24.546(5)	16.496(3)
b, Å	13.129(2)	13.135(2)	17.525(2)	15.923(5)	19.905(4)	19.506(4)	16.626(3)	17.369(3)
c, Å	19.593(2)	17.009(2)	23.440(2)	23.831(3)	23.251(4)	22.733(4)	34.071(5)	21.446(5)
α, deg	98.47(2)	67.35(2)	90	90	90	87.20(2)	90	98.12(2)
β, deg	100.51(2)	74.81(2)	90	109.36(2)	103.79(2)	89.21(2)	91.21	104.73(2)
γ, deg	116.52(2)	81.47(2)	90	90	90	73.29(2)	90	100.72(2)
V, Å^3	2709.5(10)	2552.1(1)	7103.3(13)	6354(2)	6605(2)	5504(2)		5723(2)
Z	2	2	4	4	4	4	4	2
fw	1061.1	1050.0	1389.5	1322.0	1270.3	1051.5	2694.8	2356.4
space group	$P\bar{1}$ (No. 2)	$P\bar{1}$ (No. 2)	$P2_12_12_1$ (No. 18)	$P2_1/n$ (No. 14)	$P2_1/n$ (No. 14)	$P\bar{1}$ (No. 2)	$P2_1/c$ (No. 14)	$P\bar{1}$ (No. 2)
t, °C	−130	−73	−130	−130	−130	22	−130	−130
λ, Å	0.710 69	0.710 69	0.710 69	0.710 69	0.710 69	0.710 69	0.710 69	0.710 69
ρ_{calcd}, g cm^{-3}	1.301	1.371	1.299	1.382	1.277	1.269	1.288	1.368
μ, cm^{-1}	22.21	23.56	17.17	22.88	18.35	21.84	17.49	21.12
transmissn coeff	0.981−1.000	0.994−1.000	0.996−1.000	0.939−1.000	0.981−1.000	0.988−1.000	0.983	0.967−1.000
R1[a,b]	0.069	0.059	0.041 [0.055]	0.064	0.064	0.060	0.063	0.048
wR2[c]	0.180	0.163	0.104 [0.135]	0.144	0.162	0.139	0.140	0.132
GOF	1.049	1.075	1.105	1.156	1.100	1.163	1.080	1.049
N(obsd)[d]	8263	7118	13 118	9189	9523	8737	12 119	18 760
N(indep)[e]	9287	10 396	13 728	12 787	14 013	14 537	22 164	23 153
N(refinement)[f]	8913	9904	13 447	9189	9523	8737	12 119	18 760
no. of variables	580	589	783	690	732	1100	1575	1354

[a] Calculated on the unique observed data having $I > 2\sigma(I)$ for **3**, **4**, **7**, **10**, **12**, **17**, and **18**; $I > 3\sigma(I)$ for **8**. [b] Values in brackets refer to the "inverted" structure. [c] Calculated on the unique data with $I > 0$ for **3**, **4**, and **7**, with $I > 2\sigma(I)$ for **10**, **12**, **17**, and **18**, and with $I > 3\sigma(I)$ for **8**. [d] *N*(obsd) is the total number of the independent reflections having $I > 2\sigma(I)$ for **3**, **4**, **7**, **10**, **12**, **17**, and **18** and $I > 3\sigma(I)$ for **8**. [e] *N*(indep) is the number of independent reflections. [f] *N*(refinement) is the number of reflections used in the refinement having $I > 0$ for **3**, **4**, and **7**, $I > 2\sigma(I)$ for **10**, **12**, **17**, and **18**, and $I > 3\sigma(I)$ for **8**.

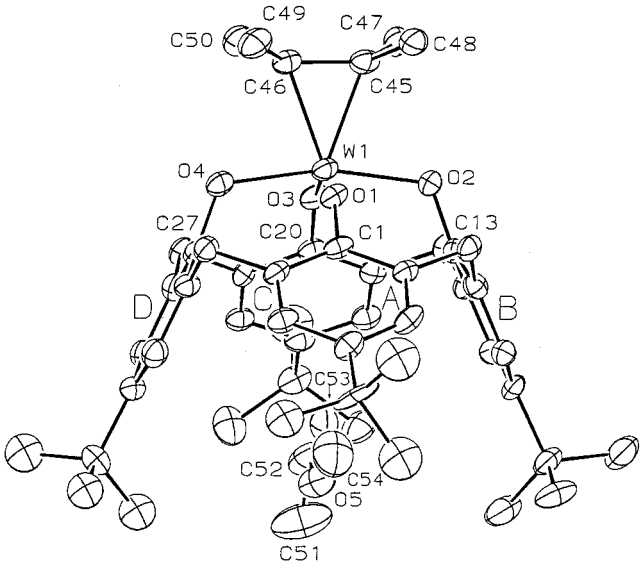

Figure 1. ORTEP drawing of complex **3** (50% probability ellipsoids). For the disordered atoms only the A position is given.

Scheme 1

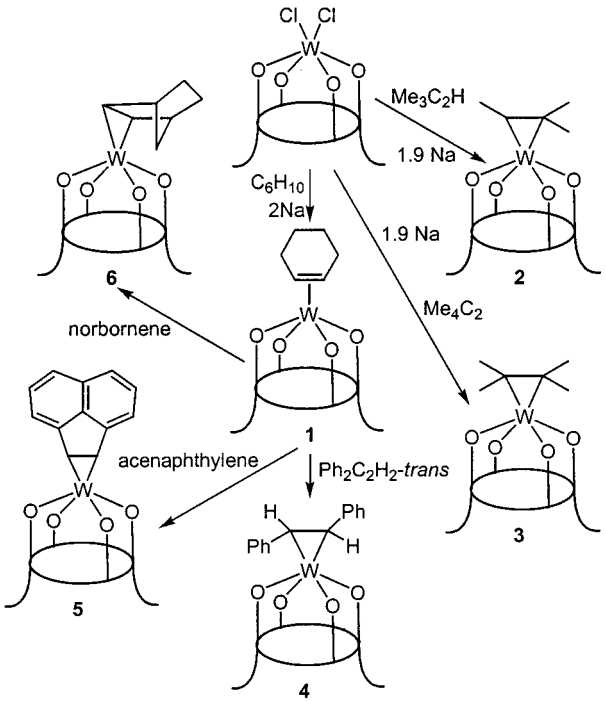

of W(IV)−calix[4]arene are easily accessible through the thermal displacement of cyclohexene from **1** using the appropriate acetylenes. The reaction led to complexes **12**−**15**. The proposed 3-metallacyclopropene has been confirmed from the spectroscopic and the X-ray data. The ^{1}H NMR data reveal a cone conformation of the calixarene with a 4-fold symmetry, for which the explanation is similar to that given for the W−alkene complexes.

The addition of the hydride to **12** via the reaction of $LiHBEt_3$ led to the 1-metallacyclopropene **10**,[9,10] which has been reported to form from the deprotonation of the stilbene complex **4**. The structure of **10**, which was not available at that time,[7b] is now reported here. The structure of the metallacyclopropenes **7**, **10**, and **12** are shown in Figures 4−6, respectively, while that of **16** is

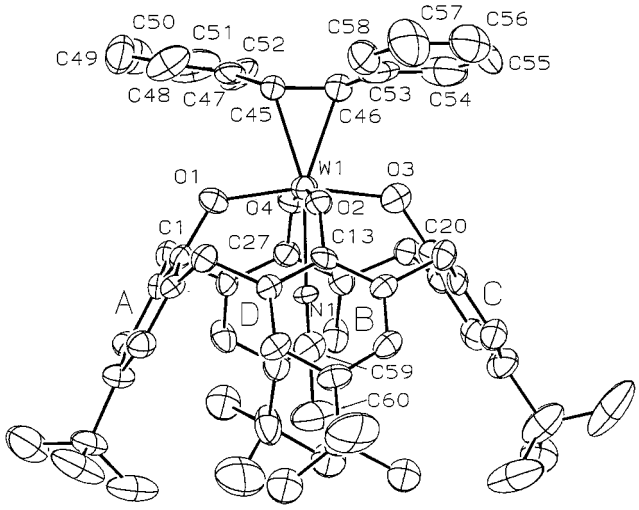

Figure 2. ORTEP drawing of complex **4** (50% probability ellipsoids). For the disordered atoms only the A position is given.

Table 2. Selected Bond Distances (Å) and Angles (deg) for Complexes 3, 4, and 8

	3	**4**	**8**
W(1)−C(45)	2.156(9)	2.178(1) [2.146(18)][a]	2.150(14) [2.163(18)]
W(1)−C(46)	2.154(8)	2.190(16) [2.14(2)]	2.168(18) [2.164(18)]
W(1)−O(1)	1.835(6)	1.941(5)	1.938(7)
W(1)−O(2)	2.022(5)	1.908(5)	1.921(6)
W(1)−O(3)	1.850(5)	1.946(6)	1.926(7)
W(1)−O(4)	2.025(6)	1.910(5)	1.925(5)
C(45)−C(46)	1.476(13)	1.37(2) [1.41(3)]	1.47(3) [1.46(2)]
Sn−C(45)			2.171 [2.238(18)]
C(45)−W(1)−C(46)	40.1(3)	38.5(8) [36.5(5)]	39.5(7) [39.9(6)]
W(1)−C(45)−C(46)	69.9(5)	72.2(8) [70.5(15)]	70.7(8) [70.3(10)]
W(1)−C(46)−C(45)	70.1(4)	71.3(8) [71.0(12)]	69.4(8) [70.2(10)]

[a] The values in brackets refer to the disordered B position.

Table 3. Selected Bond Distances (Å) and Angles (deg) for Complexes 7, 10, and 12

			12	
	7	**10**	A	B
W(1)−C(45)	2.169(6)	2.174(6)	2.031(14)	2.046(11)
W(1)−C(46)	1.916(5)	1.912(6)	2.039(12)	2.039(13)
W(1)−O(1)	1.966(4)	1.924(5)	1.879(9)	1.828(9)
W(1)−O(2)	2.021(3)	1.931(4)	1.982(8)	2.022(9)
W(1)−O(3)	1.960(4)	1.961(5)	1.852(9)	1.862(9)
W(1)−O(4)	2.011(3)	2.054(4)	1.978(9)	1.979(9)
C(45)−C(46)	1.428(7)	1.438(10)	1.326(19)	1.28(2)
C(45)−W(1)−C(46)	40.3(2)	40.6(2)	38.0(5)	36.6(6)
W(1)−C(45)−C(46)	60.3(3)	59.9(3)	71.3(8)	71.4(8)
W(1)−C(46)−C(45)	79.4(3)	79.6(4)	70.6(8)	72.0(9)

reported in the Supporting Information. The bond lengths (Table 3) within the metallacyclopropene units support the proposed bonding sequence. In all structures, the W−C single bonds are longer than 2.0 Å, though there is a significant difference between the metal binding to sp^3 (complexes **7** and **10**) or sp^2 carbons (complex **12**). The W−C46 bond distances in **7** and **10**, 1.916(5) and 1.912(6) Å, respectively, are in agreement with the presence of the 1-metallacyclopropene func-

Table 4. Selected Bond Distances (Å) and Angles (deg) for Complexes 17 and 18

	17		18	
	A	B	A	B
W(1)−O(1)	1.927(8)	1.943(7)	1.856(4)	1.850(4)
W(1)−O(2)	2.014(7)	2.023(7)	1.962(4)	1.982(3)
W(1)−O(3)	1.934(7)	1.952(7)	1.849(4)	1.848(4)
W(1)−O(4)	1.942(7)	1.925(7)	1.983(4)	1.982(3)
W(1)−C(45)	1.918(10)	1.903(10)	1.921(5)	1.914(5)
C(45)−C(46)	1.585(14)	1.575(14)	1.557(8)	1.555(7)
C(45)−C(49)	1.459(14)	1.475(15)	1.473(7)	1.472(7)
C(46)−C(47)	1.509(14)	1.551(16)	1.533(7)	1.523(6)
C(46)A−C(46)B	1.532(15)		1.551(5)	
W(1)−C(45)−C(49)	127.4(8)	128.0(7)	125.8(4)	126.9(4)
W(1)−C(45)−C(46)	125.6(7)	126.4(7)	125.3(4)	125.0(3)
C(46)−C(45)−C(49)	107.0(8)	105.5(8)	108.1(4)	107.8(4)
C(45)−C(46)−C(47)	103.1(8)	103.9(8)	102.6(4)	102.8(4)
C(45)A−C(46)A−C(46)B	112.9(8)		113.4(4)	
C(47)A−C(46)A−C(46)B	114.9(9)		114.2(4)	
C(46)A−C(46)B−C(45)B	113.8(9)		112.5(4)	
C(46)A−C(46)B−C(47)B	114.7(8)		115.4(4)	

Table 5. Comparison of Relevant Conformational Parameters within the [W(calixarene)] Units for Complexes 3, 4, and 8

	3	4	8
(a) Distances (Å) of Atoms from the O_4 Mean Plane			
O(1)	−0.133(5)	0.024(6)	0.010(5)
O(2)	0.107(4)	−0.024(6)	0.016(6)
O(3)	−0.125(5)	0.027(6)	0.010(5)
O(4)	0.125(5)	−0.027(6)	0.010(5)
W	0.380(1)	0.273(1)	0.394(1)
(b) Dihedral Angles (deg) between Planar Moieties[a]			
E∧**A**	138.2(2)	118.1(2)	119.4(2)
E∧**B**	113.6(2)	117.7(2)	128.7(2)
E∧**C**	142.0(2)	122.9(2)	121.0(2)
E∧**D**	115.0(2)	122.8(2)	128.1(2)
A∧**C**	100.2(2)	118.9(2)	119.6(3)
B∧**D**	131.4(3)	119.5(2)	103.2(3)
(c) Contact Distances (Å) between *para* C Atoms of Opposite Aromatic Rings			
C(4)···C(17)	9.701(10)	8.127(13)	7.955(16)
C(10)···C(24)	7.262(13)	8.067(12)	8.793(14)

tionality. The C45−C46 bond length varies from 1.43 Å (av) in **7** and **10** to *ca*. 1.30 Å in **12** (see Table 3). Although the lithium cation is interacting at a rather short distance (2.541(13) Å) with one of the carbons of the C_2 unit in **10**, this did not affect the structural parameters mentioned above (Table 3). The presence of a lithium cation bridging one of the oxygens of the calixarene and one of the carbons of the C_2 unit strongly affects the conformation of the overall structure. The planarity of the O_4 core is completely removed in **10** (Table 6). The macrocycle assumes a nearly half-flattened conformation, where the ***A*** ring is pushed outward with respect to the cavity, thus being roughly parallel to the reference plane (Table 6). This conformation leads the ***A*** ring to form a dihedral angle of 23.2-(2)° with the C47···C52 phenyl ring. In complexes **7** and **12** the O_4 set has a planar (**7**) or slightly tetrahedral distorted arrangement (**10**). The plane of the MC_2 fragment is perpendicular to the O_4 core both in **7** and **12** (dihedral angle 91.1(2)° in **7** and 92.3(4)° in **12**). The distances of the metals out of the O_4 plane are practically the same in the two complexes (0.369(1) Å in **7** and 0.391(1) Å in **12**). The W−O bond lengths appear in pairs, with two short and two long distances (Table 3) in both compounds.[20] The structural analysis reported

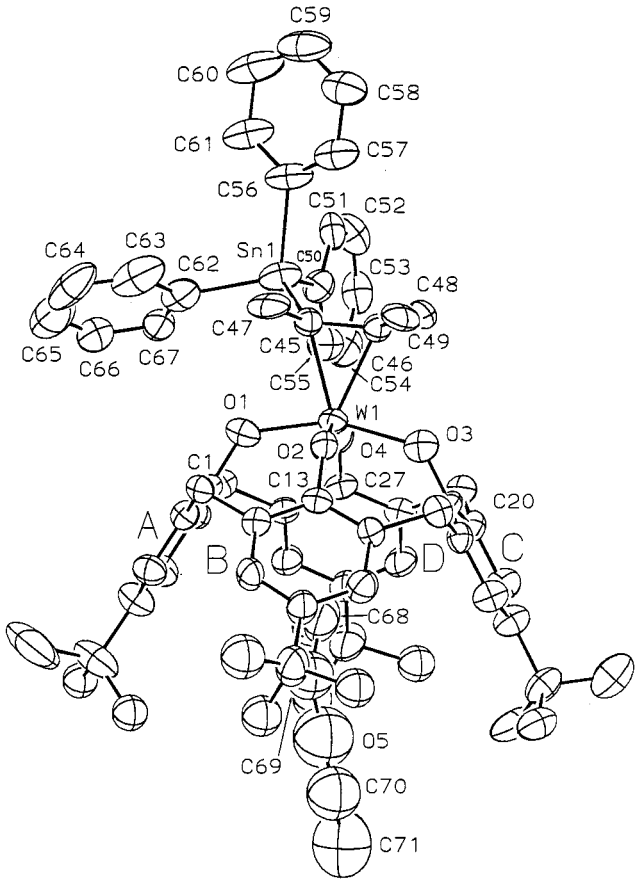

Figure 3. ORTEP drawing of complex **8** (50% probability ellipsoids). For the disordered atoms only the A position is given.

Scheme 2

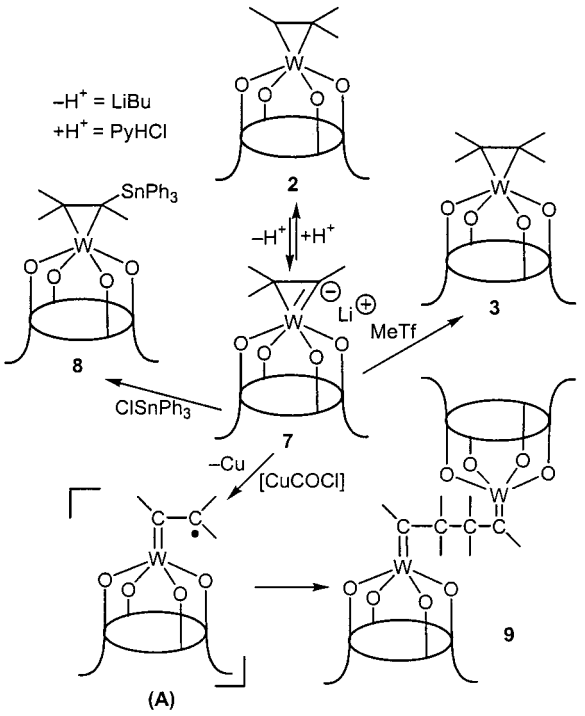

here can serve to make the comparison between the two isomeric metallacyclopropenes, namely **7** and **12**. Additional data supporting the 1-metallacyclopropene structure of **7** and **10** are (i) the pronounced high-

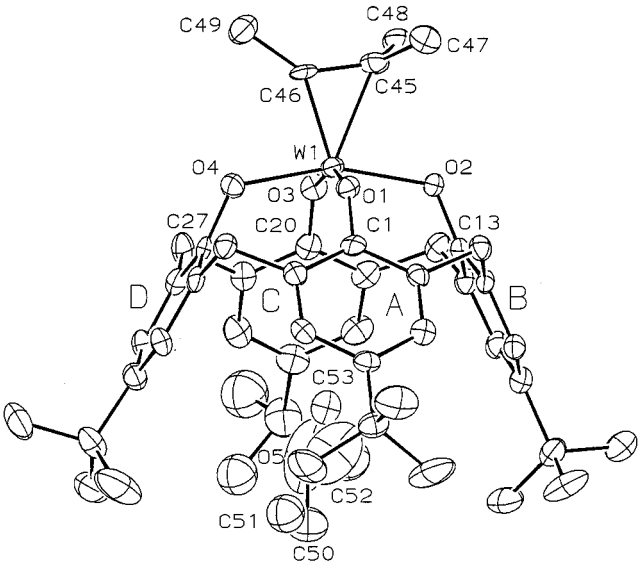

Figure 4. ORTEP drawing of the anion complex **7** (50% probability ellipsoids). For the disordered atoms only the A position is given.

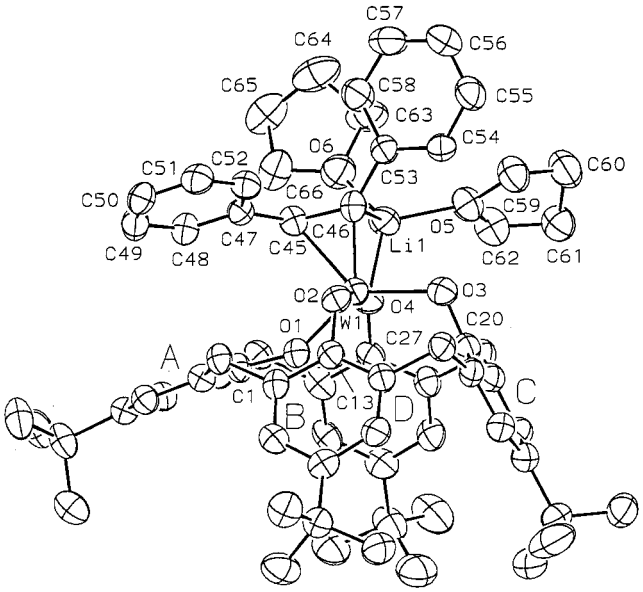

Figure 5. ORTEP drawing of complex **10** (50% probability ellipsoids).

Scheme 3

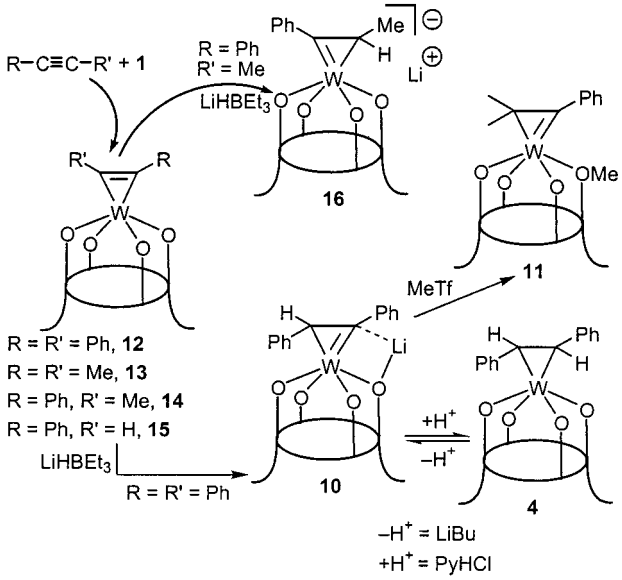

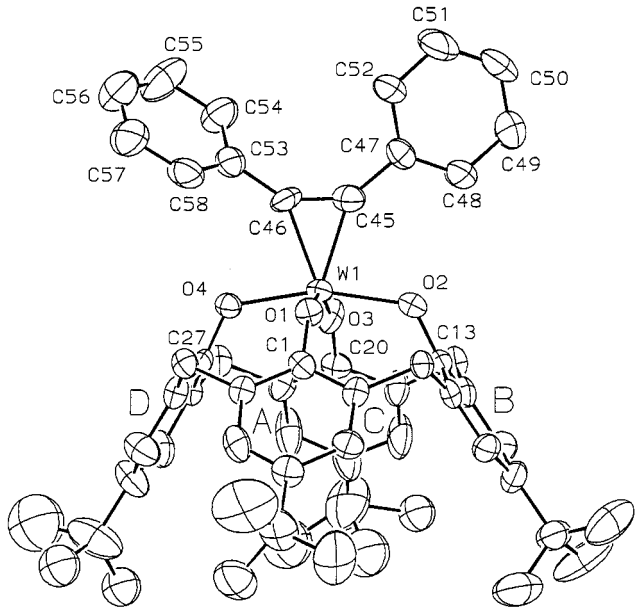

Figure 6. ORTEP drawing of molecule A of complex **12** (50% probability ellipsoids). For the disordered atoms only the A position is given.

frequency ^{13}C NMR chemical shift of the monosubstituted carbon, 271.0 and 253.1 ppm, respectively, for **7** and **10**, typical of alkylidene-like carbons and (ii) the large dihedral angles between the W1−C45−C46 and C45−C47−C48 or C45−C47−N planes, 90.0(4) and 45.80°, respectively, for **7** and **10**, which are not in agreement with a "vinyl" formulation.[9a]

There is a distinctive behavioral difference between **10** (Scheme 3) and **7** (Scheme 2) in the reaction with MeTf, which in the former case led to the alkylation of the calixarene oxygen rather than to the methylation of the 1-metallacyclopropene. The protonation of **10**, in contrast, proceeds as in the case of **7**, thus generating the *trans*-stilbene derivative **4**. The assistance of the oxygen as a primary site of the protonation can be invoked,[3,7] so that the protonation of the anionic 1-metallacyclopropene would occur via the proton transfer from the oxygen to the carbon, as supported by the DFT calculations. The solid-state structure of **10**, showing the lithium cation bridging O4 and C46 (see Figure 5), is a quite plausible structural model for the protonation of the carbon functionalities in metallacalixarene chemistry assisted by the oxygen donor atoms.

The regiochemistry of the reaction of nonsymmetric alkyne complexes with hydrides is exemplified in the reaction of **14** with $LiHBEt_3$, which leads to **16**. In other cases as well, the nucleophilic attack seems to occur at the carbon of the alkyne bearing the most electron-donating substituent. Both compounds **10** and **16** have a ^{13}C NMR resonance for the alkylidene carbon at *ca.* 250 ppm and a cone conformation of the ligand, as revealed by the ^{1}H NMR. The acenaphthylene complex,[5] when submitted to the deprotonation reaction, revealed

(20) A structural curiosity in the case of **12** is the self-assembling of the monomeric units in a zigzag chain, issued from the complexation of one of the phenyl groups of Ph_2C_2 by the calix[4]arene cavity at an adjacent monomeric unit (see the Supporting Information).

Table 6. Comparison of Relevant Conformational Parameters within the [W(calixarene)] Units for Complexes 7, 10, 12, 17, and 18

			12		17		18	
	7	**10**	A	B	A	B	A	B
			(a) Distances (Å) of Atoms from the O_4 Mean Plane					
O(1)	−0.019(4)	−0.338(4)	−0.082(8)	−0.112(8)	−0.038(7)	−0.025(7)	−0.109(4)	−0.119(4)
O(2)	0.019(4)	0.301(4)	0.084(8)	0.146(9)	0.037(7)	0.024(7)	0.110(4)	0.118(4)
O(3)	−0.019(4)	−0.276(4)	−0.123(9)	−0.102(8)	−0.036(7)	−0.030(7)	−0.109(4)	−0.117(4)
O(4)	0.020(4)	0.312(4)	0.083(8)	0.101(8)	0.037(7)	0.024(7)	0.108(4)	0.118(4)
W	0.369(1)	0.446(1)	0.391(1)	0.432(2)	0.243(1)	0.258(1)	0.374(2)	0.363(1)
			(b) Dihedral Angles (deg) between Planar Moieties[a]					
E∧**A**	126.9(1)	161.2(2)	127.2(3)	136.8(4)	132.5(3)	124.4(2)	130.5(1)	137.0(1)
E∧**B**	115.6(1)	118.2(2)	123.0(3)	120.0(3)	119.6(3)	124.2(3)	120.7(1)	120.6(1)
E∧**C**	129.0(1)	117.1(2)	134.0(3)	131.8(3)	125.4(3)	120.5(3)	132.0(1)	128.3(2)
E∧**D**	118.5(1)	120.2(2)	120.3(3)	114.5(4)	121.2(2)	124.8(3)	117.9(1)	115.9(2)
A∧**C**	104.2(2)	98.4(2)	98.7(4)	91.5(5)	102.1(4)	115.1(4)	97.5(2)	94.6(2)
B∧**D**	125.8(2)	121.4(2)	116.6(4)	125.5(4)	119.2(4)	111.0(4)	121.3(1)	123.5(2)
			(c) Contact Distances (Å) between *para* C Atoms of Opposite Aromatic Rings					
C(4)···C(17)	8.782(8)	9.231(11)	8.91(2)	9.23(2)	8.842(17)	8.253(20)	9.000(8)	9.153(9)
C(10)···C(24)	7.634(7)	7.946(10)	8.082(19)	7.54(2)	8.020(18)	8.449(17)	7.866(7)	7.748(6)

[a] **E** (reference plane) refers to the least-squares mean plane defined by the C(7), C(14), C(21), and C(28) bridging methylenic carbons.

Scheme 4

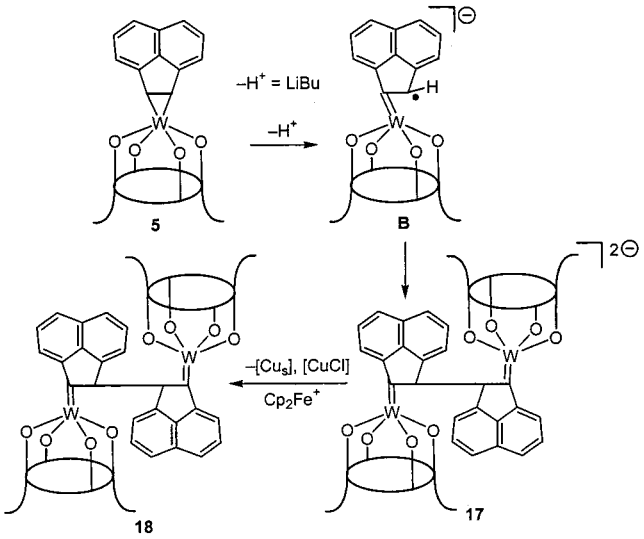

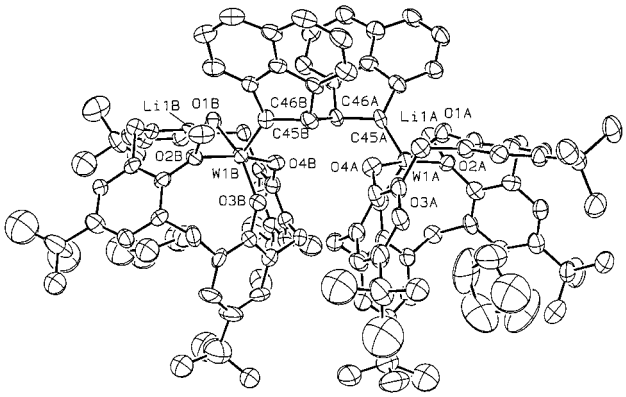

Figure 7. ORTEP drawing of complex **17** (50% probability ellipsoids). For the disordered atoms only the A and B positions are given. The THF molecules bonded to the lithium cations are omitted for clarity.

the consequence on the stability of the 1-metallacyclopropene as a function of the substituent at the olefin functionality, mainly in terms of steric constraints.

A particular instability is associated with the formation of a 1-metallacyclopropene fused with a C5 ring. As a matter of fact, the deprotonation of **5** led to the formation of **17**, via the intermediacy of **B**. It can probably be admitted that **B** originates from the homolytic cleavage of the W−C single bond of the 1-metallacyclopropene. The dimerization of **B** would lead to the dinuclear W(V) paramagnetic bis(alkylidene) shown in Scheme 4. Complex **17** undergoes either a one- or a two-electron oxidation. In the latter case the reaction, carried out using either CuCl or Cp_2FeBPh_4, led to the formation of the diamagnetic derivative **18**. The ^1H and ^{13}C NMR spectra of **18** (see Experimental Section) did not show any peculiarity or major difference with respect to the other W−alkylidene derivatives.[7a] Both complexes **17** and **18** have been structurally characterized, and a picture of their structures is shown in Figures7 and 8, respectively. They are structurally very similar, at least in the oxidation state of the metal and the presence of two lithium countercations binding at the oxygens of the calixarene in **17**. The structural parameters in Table 4 support the connectivity given in Scheme 4, with C46(A)−C46(B) distances of 1.532(15) and 1.551(5) Å in **17** and **18**, respectively. The average value of W−C45, 1.916(12) Å, shows the presence of a metalla-alkylidene functionality. The W−C45 vector is nearly parallel to the normal to the O_4 core (dihedral angles 3.1(4)° (4.3(3)°) and 2.6(2)° (0.6(1)°) for **17** and **18**, respectively), which shows significant tetrahedral distortions. Tungsten is displaced from this plane toward the C45 carbon. The geometry of the coordination polyhedron (Table 4) as well as the elliptical cone section of the macrocycle (Table 6) are in good agreement with those found in **3** and **12**. The mutual orientation of the two molecules in a dimer leads the two independent O_4 cores to be nearly perpendicular to each other (dihedral angles 91.9(4) and 97.5(1)° for **17** and **18**, respectively).

The 1-metallacyclopropene anions in Schemes 2−4 are isomers of metallaalkylidyne anions, which they rearrange to when the substituents at the two carbons of the C=C double bonds are protons. Such related species are similar in their behavior toward oxidizing agents. Their dimerization can be achieved by one-electron oxidation. In the case of alkylidynes, their

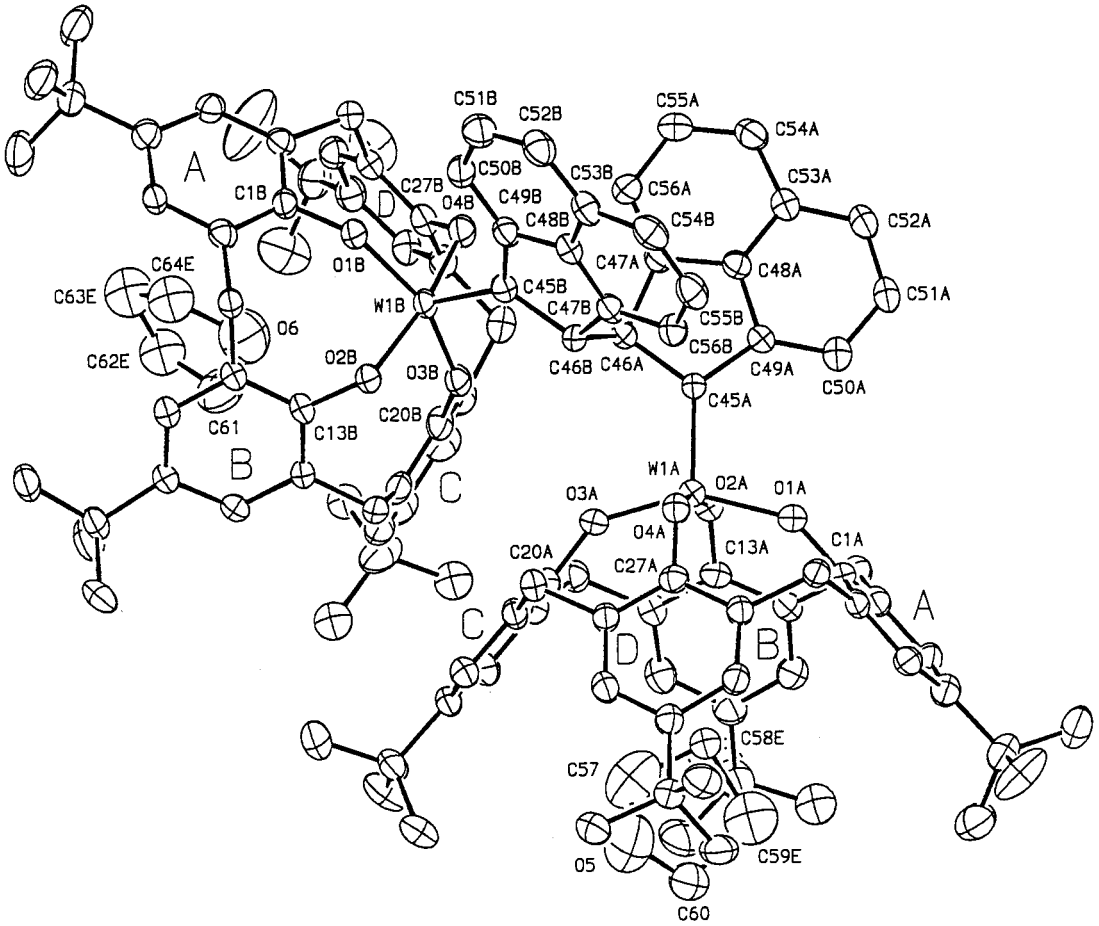

Figure 8. ORTEP drawing of complex **18** (50% probability ellipsoids). For the disordered atoms only the A and B positions are given.

dimerization led to the formation of $\mu,\eta^2{:}\eta^2$-acetylene,[7a] while in Scheme 2 we afforded the formation of a dinuclear bis(alkylidene). The alternative synthesis of the latter compounds passes through the deprotonation of strained olefins, which undergo spontaneous evolution to dinuclear alkylidenes.

(B) Theoretical Analysis: Density Functional Investigation of the 1-Metallacyclopropenes. Density functional calculations were performed to gain a better understanding of the electronic structure of the alkene, vinyl, and alkyne complexes supported by the tungsten calixarene fragment (**3**, **7**, and **12**, respectively) and to elucidate their reactivity patterns. All of the tungsten calixarene complexes have been simplified by replacing the four Bu^t groups of calixarene ligand and the organic groups of the alkene, vinyl, or alkyne moieties with hydrogen atoms to reduce the computational effort. The considered molecules, which are only slightly different from the actual complexes, will be called hereafter as **3***, **7***, and **12***, respectively. DFT calculations including nonlocal correction to the exchange-correlation potential have been shown to describe adequately the geometry of organometallic compounds.[21]

The main geometric parameters of the optimized structures for **3***, **7***, and **12*** are reported in Table 7 and compared with the experimental data, using the numbering scheme of Figures 1, 4, and 6. The optimized geometries are in good agreement with the experimental X-ray data; bond distances agree within 0.02−0.03 Å, while the largest deviation of bond angles is about 6°. In particular, the geometry calculated for **7** reproduces the 1-metallacyclopropene feature of this compound with one W−C bond shorter than the other and a rather long C−C bond. A DFT calculation has been recently performed on a [Cp(CO)$_2$Re(η^2-CHCH$_2$)] complex, with the same spectroscopic and geometric characteristics of **7** and **10**, and a subsequent natural orbital analysis (NBO) strongly supported the 1-metallacyclopropene nature of this species.[9a]

The energy barrier for the rotation of the ethylene, vinyl, and acetylene moieties around the metal−ligand axis was estimated by performing geometry optimizations under C_{2v} symmetry constraints on **3***, **7***, and **12***, with the organic fragment rotated by 45° with respect to the O(1)−W−O(3) and O(2)−W−O(4) planes. Small energy barriers were found (5.7, 1.8, and 7.3 kcal mol^{-1}, respectively), which suggest free rotation above 100 K. This is in agreement with the ^{1}H NMR of **3**, **7**, and **12**, indicating an apparent C_{4v} symmetry of the calixarene moiety.

The electron-rich anionic 1-metallacyclopropenes easily undergo reactions with electrophiles. Both charge and orbital frontier factors may determine the regiochemistry of the electrophilic attack, and charge effects are expected to prevail when hard electrophiles, such as H$^+$ and Me$^+$, are employed. The results of Mulliken population analysis on the optimized geometry of **7***

(21) (a) Ziegler, T. *Chem. Rev* **1991**, *91*, 651. (b) *Reviews in Computational Chemistry*; Lipkowitz, K. B., Boyd, D. B., Eds.; VCH: New York, 1990−1999; Vols. 1−13.

Table 7. Main Geometrical Parameters Calculated for the Model Complexes 3*, 7*, and 12* Compared with the Experimental Values for 3, 7, and 12

	theor			X-ray		
	3*	**7***	**12***	**3**	**7**	**12B**
W(1)−C(45)	2.138	2.169	2.047	2.156(9)	2.169(6)	2.046(11)
W(1)−C(46)	2.138	1.896	2.047	2.154(8)	1.916(5)	2.039(13)
W(1)−O(1) (av)	1.875	1.960	1.873	1.843(6)	1.963(4)	1.845(9)
W(1)−O(2)	1.875	2.064	2.046	2.022(5)	2.021(3)	2.022(9)
W(1)−O(4)	2.037	2.056	2.046	2.025(6)	2.011(3)	1.979(9)
C(45)−C(46)	2.037	1.433	1.305	1.476(13)	1.428(7)	1.28(2)
C(45)−W(1)−C(46)	39.8	40.6	37.8	40.1(3)	40.3(2)	36.6(6)
O(1)−W(1)−O(3)	148.4	155.3	144.9	147.9(2)	157.1(2)	145.9(4)
O(2)−W(1)−O(4)	162.5	160.4	163.7	165.0(2)	160.0(1)	162.2(4)
W(1)−O(1)−C(1) (av)	149.6	142.7	151.9	150.1(5)	134.7(3)	149.0(9)
W(1)−O(2)−C(13)	117.6	117.9	116.4	116.7(5)	122.5(3)	121.1(9)
W(1)−O(4)−C(27)	117.6	119.0	116.4	117.2(5)	125.4(3)	120.2(8)

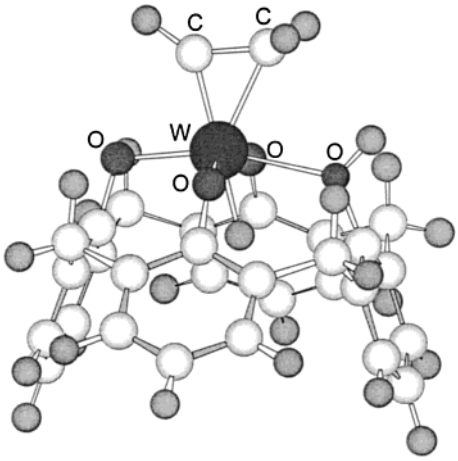

Figure 9. Optimized structure of the oxygen-protonated 1-metallacyclopropene **C**.

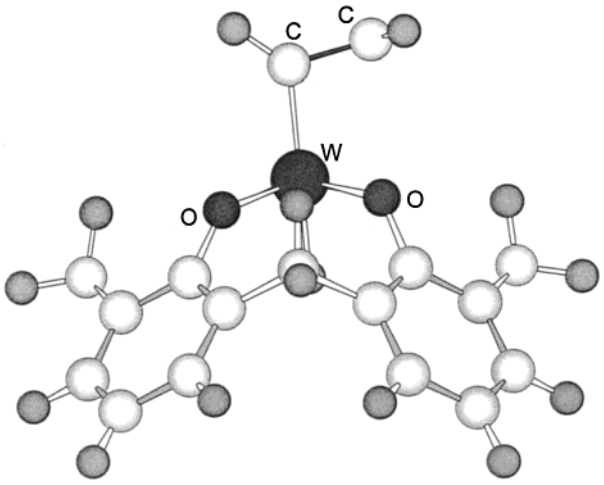

Figure 10. Optimized structure of the oxidized η^1-vinyl radical **A**.

show that the four oxygen atoms of calixarene bear the highest negative charges (−0.83/−0.87), while the monosubstituted carbon atom of the metallacyclopropene ring (C′) bears a slightly lower negative charge (−0.54). At the same time, an analysis of the frontier orbitals shows that **7*** has a high-lying isolated HOMO which is mainly localized on the C′ atom (41%). Therefore, the incoming electrophiles may attack either one of the calixarene oxygens on the basis of charge factors or the vinyl C′ atom on the basis of both charge and frontier factors. Moreover, although the negative charge on the calixarene oxygens is higher than that on the vinyl C′ atom, the difference is quite small (less than 0.30) and could be easily affected by the substituents (Me or Ph) which are present in actual complexes such as **7** and **10**. Although, due to the larger size and the lower symmetry, we could not perform any calculations on these substituted complexes, some trends can be foreseen on the basis of qualitative considerations. For instance, in **7**, where the vinyl moiety takes three electron-donating methyl groups, we expect a higher negative charge on the vinyl C′ atom so that both charge and frontier orbital factors would preferentially direct the electrophilic attack to the C′ atom, in agreement with the experimental evidence. On the other hand, in **10**, where the vinyl moiety takes two phenyl groups, we expect the charges of the oxygen and C′ atoms to be close to those calculated for **7*** with a higher charge on the oxygen atoms, so that this complex would preferentially undergo the electrophilic attack at one of the calixarene oxygens. This is in agreement with the regiochemistry of the alkylation of **10** but not with the regiochemistry of the protonation which is directed at the vinyl C′ atom. However, the regiochemistrry of the protonation may be determined by the high mobility of the proton that could easily migrate from the oxygen to the C′ atom giving the thermodynamically most stable product, which is expected to be the olefin complex.

To clarify this point, we have compared the energies of the two products resulting from the proton attack on the vinyl C′ atom or on one of the calixarene oxygens (the one bearing the highest negative charge) of **7***. The former product is simply the ethylene complex **3***, which has already been theoretically characterized. The latter product is the neutral oxygen-protonated metallacyclopropene **C** (Figure 9), for which a full geometry optimization under C_s symmetry constraints has been performed. The C′-protonated ethylene complex has been calculated to be 46 kcal mol^{-1} more stable that the O-protonated 1-metallacyclopropene, thus supporting our hypothesis.

We finally considered the one-electron oxidation of the 1-metallacyclopropene **7** leading to the dimeric species **9**. An analysis of the frontier orbitals of **7*** (see above) has shown the presence of a high-lying isolated HOMO, which is mainly localized on the C′ atom. The removal of one electron from **7*** is therefore expected to lead to a C′-centered radical, as confirmed by a single-point DFT calculation of **7***$^+$ using the optimized geometry

of **7***, which shows that the singly occupied molecular orbital (SOMO) is mainly localized on the vinyl C′ atom (61%) and gives a low vertical ionization energy, 71 kcal mol^{-1}. A first geometry optimization of $\mathbf{7}^{*+}$ leads to a slightly relaxed structure with elongated W−C bond lengths. However, a lower energy minimum (by 7 kcal mol^{-1}) was found for a structure with the W−C bond at the most substituted carbon homolytically cleaved, thus corresponding to an η^1-vinyl radical (Figure 10). This result supports the mechanism proposed in Scheme 2 based on the intermediacy of the free radical species **A**.

Acknowledgment. We thank the "Fonds National Suisse de la Recherche Scientifique" (Bern, Switzerland; Grant No. 20-53336.98), Action COST D9 (European Program for Scientific Research, OFES No. C98.008), and Fondation Herbette (University of Lausanne, N.R.) for financial support.

Supporting Information Available: ORTEP and SCHAKAL diagrams, details of the X-ray data collection, structure solution, and refinement, and tables giving crystal data and structure refinement details, atomic coordinates, isotropic and anisotropic displacement parameters, and bond lengths and angles for **3**, **4**, **7**, **8**, **10**, **12**, **17**, and **18** and SCHAKAL drawings, crystal data, and tables giving crystal data and structure refinement details, atomic coordinates, isotropic and anisotropic displacement parameters, and bond lengths and angles for **6** and **16**. This material is available free of charge via the Internet at http://pubs.acs.org.

OM0006155